

## Two-channel totally asymmetric simple exclusion processes

To cite this article: Ekaterina Pronina and Anatoly B Kolomeisky 2004 *J. Phys. A: Math. Gen.* **37** 9907

View the [article online](#) for updates and enhancements.

### You may also like

- [Non-equilibrium statistical mechanics: from a paradigmatic model to biological transport](#)  
T Chou, K Mallick and R K P Zia
- [Spectrum of the totally asymmetric simple exclusion process on a periodic lattice—first excited states](#)  
Sylvain Prohac
- [The effect of unequal constrained at branching point on phase diagrams](#)  
Song Xiao, Xiaoyu Chen and Yanna Liu

# Two-channel totally asymmetric simple exclusion processes

**Ekaterina Pronina and Anatoly B Kolomeisky**

Department of Chemistry, Rice University, Houston, TX 77005-1892, USA

E-mail: tolya@rice.edu

Received 9 July 2004, in final form 23 August 2004

Published 6 October 2004

Online at [stacks.iop.org/JPhysA/37/9907](http://stacks.iop.org/JPhysA/37/9907)

doi:10.1088/0305-4470/37/42/005

## Abstract

Totally asymmetric simple exclusion processes, consisting of two coupled parallel lattice chains with particles interacting with hard-core exclusion and moving along the channels and between them, are considered. In the limit of strong coupling between the channels, the particle currents, density profiles and a phase diagram are calculated exactly by mapping the system into an effective one-channel totally asymmetric exclusion model. For intermediate couplings, a simple approximate theory, that describes the particle dynamics in vertical clusters of two corresponding parallel sites exactly and neglects the correlations between different vertical clusters, is developed. It is found that, similarly to the case of one-channel totally asymmetric simple exclusion processes, there are three stationary state phases, although the phase boundaries and stationary properties strongly depend on inter-channel coupling. Extensive computer Monte Carlo simulations fully support the theoretical predictions.

PACS numbers: 05.70.Ln, 05.60.Cd, 02.50.Ey, 02.70.Uu

## 1. Introduction

In recent years asymmetric simple exclusion processes (ASEPs) have become an important tool of investigation for many processes in chemistry, physics and biology [1, 2]. ASEPs have been applied successfully to understand the kinetics of biopolymerization [3], polymer dynamics in dense media [4], diffusion through membrane channels [5], gel electrophoresis [6], dynamics of motor proteins moving along rigid filaments [7] and the kinetics of synthesis of proteins [8–10].

ASEPs are one-dimensional lattice models where particles interact only with hard-core exclusion potential. Each lattice site can be occupied by a particle or it can be empty. In the simplest totally asymmetric simple exclusion process (TASEP), where the particles can only

move in one direction, the dynamic rules are as follows. The particle at site  $i$  can jump forward to the site  $i + 1$  with the rate 1 if the target site is empty. The particle can enter the lattice with the rate  $\alpha$ , provided the first site is unoccupied, and it can also leave the system with the rate  $\beta$ . Although these dynamic rules are very simple, they lead to a very rich and complex dynamic phase behaviour. There are non-equilibrium phase transitions between the stationary states of the system, induced by boundary processes, that have no analogues in equilibrium systems [1, 2, 11].

The coupling of ASEPs with different equilibrium and non-equilibrium processes has led to many unusual and unexpected phenomena. The introduction of a single irreversible detachment process to the bulk of the system has resulted in significant changes in the phase diagram [13]. The coupling of ASEPs with equilibrium Langmuir kinetics at each site produced unusual phenomena of localized density shocks [12, 14–16]. However, the complexity of phase transitions in ASEPs can be explained and understood reasonably well by applying a phenomenological domain-wall theory [2, 11].

Most investigations of ASEPs concentrate on one-channel systems where particles can only move along one lattice chain. However, the description of many real phenomena would be more adequate if parallel-chain asymmetric exclusion processes were used. For example, motor proteins kinesins can move along the parallel protofilaments of microtubules, and there are no restrictions for them to jump between these protofilaments [17]. Parallel-chain ASEPs have been considered earlier [18–20]. However, in these investigations the coupling between different chains was indirect, i.e., hopping between the chains was forbidden. The aim of the present paper is to investigate two-chain asymmetric exclusion processes, where particles can move between the lattice channels. We investigate this system by using a simple approximate model for intermediate couplings and by mapping it to exactly solved one-channel TASEPs in the limits of strong coupling and no coupling. In addition, extensive computer Monte Carlo simulations are performed in order to validate theoretical predictions.

The paper is organized as follows. In section 2 we give a detailed description of the model, discuss known results for one-channel ASEPs, solve exactly the stationary state properties of the system in the limit of strong coupling, and develop an approximate theory for two-channel asymmetric exclusion processes for intermediate couplings. Then in section 3 we present and discuss Monte Carlo simulations results. Finally, we summarize and conclude in section 4.

## 2. Theoretical description of a two-channel TASEP

### 2.1. Model

We consider identical particles moving on two parallel one-dimensional lattices, each lattice having  $L$  sites, as shown in figure 1. The dynamics in the system is random sequential, i.e., at every time step we randomly choose a site in one of the lattices. Every site on both lattices can be either empty or occupied by no more than one particle. In the bulk of the system the dynamic rules are as follows. A particle at site  $i$  can hop up or down to the same site  $i$  on the other lattice chain with the rate  $0 \leq w \leq 1$ , if that site is empty. The particle can also move from left to right along the same lattice to site  $i + 1$ , if this site is available. However, this transition rate depends on occupation of site  $i$  at the neighbouring channel. If there is no particle at that site, the rate is equal to  $1 - w$ , otherwise the particle jumps with the rate 1 (see figure 1). It means that the full transition rate of leaving site  $1 \leq i < L$ , to go forward or up/down, is always equal to 1. This can be easily understood by recalling that the transition rate is a probability of transition per unit time step. Particles can also enter the system with the rate  $\alpha$  if any of the first sites in either channel are empty. When a particle reaches site  $L$ , it

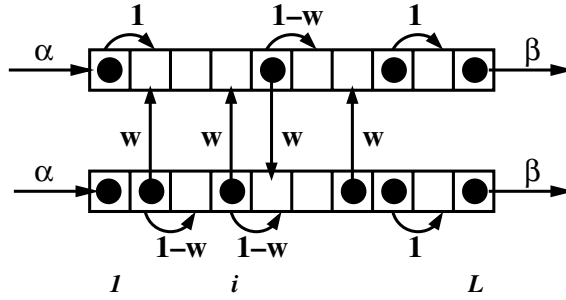


**Figure 1.** Schematic view of the model for a two-channel TASEP. Allowed transitions are shown by arrows. Inter-channel hopping rates are equal to  $w$ . The transition rates to move along the channel are  $1 - w$ , if there is no particle at the same site in another channel, otherwise it is equal to 1. Entrance and exit rates are  $\alpha$  and  $\beta$  (or  $\beta(1 - w)$  if the last cluster is half-empty), respectively, and are the same in both channels.

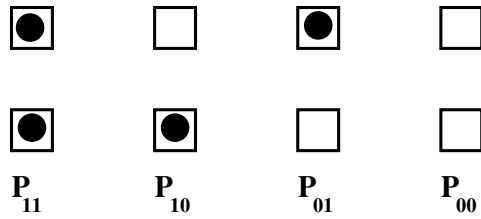


**Figure 2.** Four possible states for a vertical cluster of lattice sites.  $P_{11}$ ,  $P_{10}$ ,  $P_{01}$  and  $P_{00}$  are the corresponding probabilities for each state.

can exit with the rate  $\beta$ , when both last sites are occupied, or with the rate  $\beta(1 - w)$  if there is no vertical neighbour at the other lattice chain.

When a vertical transition rate  $w = 0$ , we have two uncoupled single-channel totally asymmetric simple exclusion processes for which an exact description of phase diagram, density profiles and particle currents is known [1, 2]. In this case there are three steady-state phases, determined by the processes at the boundaries or in the bulk of the system. For  $\alpha > 1/2$  and  $\beta > 1/2$ , the particle dynamics is specified by the processes in the bulk of the system, and we have a maximal-current phase with the following stationary current and bulk density:

$$J_{MC} = \frac{1}{4}, \quad \rho_{\text{bulk,MC}} = \frac{1}{2}. \tag{1}$$

The entrance into the system determines the overall particle dynamics for  $\alpha < \beta$  and  $\alpha < 1/2$ . In this case, the system can be found in a low-density phase with the current and bulk density given by

$$J_{LD} = \alpha(1 - \alpha), \quad \rho_{\text{bulk,LD}} = \alpha. \tag{2}$$

When the exit from the system limits the overall dynamics, which takes place for  $\beta < \alpha$  and  $\beta < 1/2$ , the system exists in a high-density phase. In this case, the current and bulk densities are equal to

$$J_{HD} = \beta(1 - \beta), \quad \rho_{\text{bulk,HD}} = 1 - \beta. \tag{3}$$

For vertical transition rates  $w > 0$ , the particle dynamics in both channels depend on each other, and any successful theoretical description should be able to account for this coupling. Let us consider a cluster of two vertical sites  $i$ . There are four possible states for this cluster, as shown in figure 2.  $P_{11}^{(i)}$  is defined as a probability to find a cluster with both lattice sites

occupied. Then  $P_{10}^{(i)}$  and  $P_{01}^{(i)}$  are the probabilities that only lower or upper channel site is occupied (see figure 2). Finally,  $P_{00}^{(i)}$  is a probability that both sites in the cluster are empty. The normalization condition for these probabilities gives us

$$P_{11}^{(i)} + P_{10}^{(i)} + P_{01}^{(i)} + P_{00}^{(i)} = 1. \quad (4)$$

In the bulk of the system at stationary state, it is reasonable to expect that these probabilities are independent of the position of the vertical cluster due to the symmetry. In what follows, we omit the superscript  $i$  for bulk values of these probabilities since only steady-state processes will be considered. Also, because both channels are equivalent, we expect that  $P_{10}^{(i)} = P_{01}^{(i)}$ . Then the bulk density at each lattice chain, which is also independent of the position on the lattice in stationary state limit, is given by

$$\rho = P_{11} + P_{10}. \quad (5)$$

Thus the overall dynamics of the system can be fully described in terms of these probabilities.

## 2.2. Strong-coupling limit

In the limit of strong coupling ( $w = 1$ ), the dynamics of the system simplifies significantly, because at large times any vertical cluster cannot exist in a configuration where both sites are empty, i.e.,  $P_{00} = 0$ . This can be seen from the following arguments. A vertical cluster in state  $\{00\}$  could only be obtained by moving particle along the corresponding lattice chain if the previous state of the same cluster was  $\{10\}$  or  $\{01\}$ . However, the rate for this transition in the limit of strong coupling is equal to  $1 - w = 0$ , and the configuration  $\{00\}$  can never be reached for any vertical cluster. Thus, in this system there are only two types of clusters: fully filled and half-filled. One can think of filled clusters as new effective ‘particles’ and half-filled clusters then can be viewed as new effective ‘holes’. The two-channel TASEP in this limit can be mapped into the one-channel totally asymmetric exclusion process with the effective entrance rate  $\alpha$  and the effective exit rate  $2\beta$ . In the bulk of the system an effective new particle jumps to the right with rate 1, if this move is allowed. The factor 2 in the effective exit rate is due to the fact that there are two ways of leaving the system from the filled cluster at last site, namely, by moving particles from the upper or lower lattice channels.

The exact density profiles, particle currents and phase diagram for this effective one-channel TASEP system are known [1, 2], and it allows us to calculate exactly the properties of the original two-channel TASEP in the limit of strong coupling. The steady-state particle current of the effective one-channel model  $J^*$  is related to the particle current per channel  $J$  of the original two-channel model in the following way,

$$J = \frac{J^*}{2}, \quad (6)$$

while using equation (5) we obtain the corresponding relation for bulk density profiles in the two-channel TASEP,

$$\rho = \rho^* + (1 - \rho^*)/2 = (1 + \rho^*)/2, \quad (7)$$

where  $\rho^*$  is the effective density for one-channel asymmetric exclusion model.

Thus we conclude that there are three stationary state phases for the two-channel TASEP in the limit of strong coupling. When  $\alpha < 2\beta$  and  $\alpha < 1/2$ , the system can be found in the low-density phase with the following properties:

$$P_{11,LD} = \alpha, \quad P_{10,LD} = (1 - \alpha)/2, \quad J_{LD} = \alpha(1 - \alpha)/2, \quad \rho_{\text{bulk,LD}} = (1 + \alpha)/2. \quad (8)$$

The conditions  $\alpha > 2\beta$  and  $\beta < 1/4$  specify the high-density phase. In this case, the steady-state properties are given by

$$P_{11,\text{HD}} = 1 - 2\beta, \quad P_{10,\text{HD}} = \beta, \quad J_{\text{HD}} = \beta(1 - 2\beta), \quad \rho_{\text{bulk,HD}} = 1 - \beta. \quad (9)$$

In the case, when bulk dynamics is rate-limiting, we have the maximal-current phase with the following parameters:

$$P_{11,\text{MC}} = \frac{1}{2}, \quad P_{10,\text{MC}} = \frac{1}{4}, \quad J_{\text{MC}} = \frac{1}{8}, \quad \rho_{\text{bulk,MC}} = \frac{3}{4}. \quad (10)$$

### 2.3. Approximate solutions for intermediate couplings

For intermediate couplings,  $0 < w < 1$ , any vertical cluster can exist in all four possible states and we cannot map the two-channel TASEP into the effective one-channel model. Some reasonable approximations are needed in order to calculate the steady-state properties of the system.

Assume that a state of a given vertical cluster is independent of states of its neighbours. It means that the cluster dynamics is considered in a mean-field description. Then the probability of finding the cluster at the position  $i$  with both sites occupied changes in time as given by

$$\frac{dP_{11}}{dt} = P_{11}(P_{10} + P_{01}) + 2(1 - w)P_{10}P_{01} - 2P_{11}P_{00} - P_{11}(P_{10} + P_{01}), \quad (11)$$

where the first term corresponds to the probability density flux from sites  $i - 1$ , the second term describes the changes at both sites  $i$  that lead to the formation of the cluster  $\{11\}$ , and two negative terms represent the density flux leaving from sites  $i$ . This equation describes the dynamics of the occupied vertical cluster for any configurations of neighbouring clusters. Applying the symmetry relation  $P_{10} = P_{01}$  at large times simplifies this expression into

$$0 = (1 - w)P_{10}^2 - P_{11}P_{00}. \quad (12)$$

This equation, with the help of the normalization condition (4), yields

$$P_{10} = \frac{-P_{11} + \sqrt{P_{11}^2 + (1 - w)P_{11}(1 - P_{11})}}{1 - w}. \quad (13)$$

This rather complex relation can take a simpler form for two limiting cases—for the two-channel TASEP without coupling and in the strong-coupling limit. For  $w = 0$  we obtain

$$P_{10} = \sqrt{P_{11}} - P_{11}, \quad (14)$$

while for  $w = 1$  it transforms into

$$P_{10} = \frac{1 - P_{11}}{2}, \quad (15)$$

in agreement with exact calculations presented above (see equations (8)–(10)).

The particle current per channel can be written as

$$J = [P_{11} + (1 - w)P_{10}](1 - P_{10} - P_{11}). \quad (16)$$

In this expression, the first multiplier gives the probability to find a vertical cluster in configurations, from which the particle can hop to the right, while the second multiplier gives the probability that the site ahead is available. Using relation (13) we can express the particle current only in terms of one variable, the density of vertical clusters  $P_{11}$ ,

$$J = \sqrt{P_{11}(1 - w + wP_{11})} \frac{1 - w + wP_{11} - \sqrt{P_{11}(1 - w + wP_{11})}}{1 - w}. \quad (17)$$

Again, simpler relations can be obtained for two limiting cases of zero coupling and strong coupling. The particle current in the case of  $w = 0$  is given by

$$J = \sqrt{P_{11}}(1 - \sqrt{P_{11}}), \tag{18}$$

while for  $w = 1$  we conclude that

$$J = \frac{P_{11}(1 - P_{11})}{2}. \tag{19}$$

These relations also agree with exact results discussed above.

We expect that, similarly to the case of zero inter-channel coupling or in the strong-coupling limit, there are three possible stationary phases. The conditions for a maximal-current phase can be specified by computing a maximum of the particle current as a function of density of  $\{11\}$  clusters, i.e.,  $\frac{\partial J}{\partial P_{11}} = 0$ . It leads to the following equation:

$$\frac{[1.5w\sqrt{P_{11}}(1 - w + wP_{11}) + \frac{(1-w+wP_{11})^{1.5}}{2\sqrt{P_{11}}} - 1 + w - 2wP_{11}]}{1 - w} = 0. \tag{20}$$

For any value of inter-channel coupling  $w$  this equation can always be solved exactly numerically, and we can obtain the value of the density of filled vertical clusters in the maximal-current phase. Because this equation can have more than one real solution, we should always choose the physically reasonable solution which gives  $1/4 < P_{11,MC} < 1/2$ . Utilizing equations (5), (13) and (17), the stationary properties of this phase can be easily determined. For example, for  $w = 0.5$  the calculations show that

$$P_{11,max} \simeq 0.317, \quad P_{10,max} \simeq 0.280, \quad \rho_{bulk,max} \simeq 0.597, \quad J_{max} \simeq 0.184. \tag{21}$$

In the low-density phase, the entrance rate  $\alpha$  limits the overall particle dynamics, and the expression for the current per channel is given by

$$J_{LD} = \alpha(1 - P_{11} - P_{10}), \tag{22}$$

or, using equation (13), it can be written as

$$J_{LD} = \alpha \frac{1 - w + wP_{11} - \sqrt{P_{11}}(1 - w + wP_{11})}{1 - w}. \tag{23}$$

Comparing this equation with the expression for the particle current in the bulk of the system (see equation (17)), it can be shown that

$$\alpha = \sqrt{P_{11}}(1 - w + wP_{11}), \tag{24}$$

from which the value of density of  $\{11\}$  clusters in the low-density phase can be obtained as follows:

$$P_{11,LD} = \frac{-1 + w + \sqrt{(1 - w)^2 + 4w\alpha^2}}{2w}. \tag{25}$$

Applying again equation (13), we derive the expression for the density of  $\{10\}$  clusters,

$$P_{10,LD} = \frac{\alpha}{1 - w} + \frac{1 - \sqrt{1 + w \left(\frac{2\alpha}{1-w}\right)^2}}{2w}. \tag{26}$$

These equations allow us to calculate the bulk density as  $\rho = P_{11} + P_{10}$ , and also, substituting equation (25) into equation (23), the particle current per channel can be expressed as

$$J_{LD} = \frac{\alpha}{2} \left[ 1 - \frac{2\alpha}{1 - w} + \sqrt{1 + 4w \left(\frac{\alpha}{1 - w}\right)^2} \right]. \tag{27}$$

When exit dynamics determines the overall behaviour of the system we have a high-density phase. The particle current per channel is given by

$$J_{\text{HD}} = \beta[P_{11} + (1 - w)P_{10}], \quad (28)$$

and, after applying equation (13), it transforms into

$$J_{\text{HD}} = \beta\sqrt{P_{11}(1 - w + wP_{11})}. \quad (29)$$

Again comparing this expression with the particle current in the bulk, as given by equation (17), we derive the density of filled vertical clusters,

$$P_{11,\text{HD}} = 1 - \beta - \frac{1 - \sqrt{1 - 4w\beta(1 - \beta)}}{2w}. \quad (30)$$

Substitution of it into equation (13) allows us to compute the density of  $\{10\}$  clusters,

$$P_{10,\text{HD}} = \frac{1 - \sqrt{1 - 4w\beta(1 - \beta)}}{2w}. \quad (31)$$

Then the bulk density in each channel is equal to  $\rho_{\text{HD}} = P_{11,\text{HD}} + P_{10,\text{HD}} = 1 - \beta$ . It is interesting to note that the bulk density in this phase is always independent of inter-channel coupling and depends only on exit rate, although the densities of filled and half-filled clusters strongly depend on  $w$ . The expression for the particle current can be derived from equations (29) and (30),

$$J_{\text{HD}} = \frac{\beta}{2}[1 - 2\beta + \sqrt{1 - 4w\beta(1 - \beta)}]. \quad (32)$$

There are two types of phase transitions in the system. The boundary between the low-density and high-density phases specifies the first-order phase transition with jumps in bulk densities, while the transition between the maximal-current and low-density or high-density phase is continuous. The low-density and high-density phases coexist when the particle currents in each phase are equal, i.e.,  $J_{\text{HD}} = J_{\text{LD}}$ . From equations (27) and (32) we obtain

$$\frac{\alpha}{2} \left[ 1 - \frac{2\alpha}{1 - w} + \sqrt{1 + 4w \left( \frac{\alpha}{1 - w} \right)^2} \right] = \frac{\beta}{2} [1 - 2\beta + \sqrt{1 - 4w\beta(1 - \beta)}], \quad (33)$$

which determines the phase boundary curve in  $\{\alpha, \beta\}$ -coordinates. One can observe that, in contrast to the systems with zero coupling or in the limit of strong coupling, the phase boundary here is not a linear function of parameters. Similar arguments can also be used to find the boundaries between the low-density or high-density and the maximal-current phases. Theoretically, calculated phase diagrams for different inter-channel couplings are presented in figure 3.

### 3. Monte Carlo simulations and discussions

Our approximate theory treats exactly the particle dynamics inside vertical clusters, however, interactions between the clusters are accounted for in an approximate mean-field fashion. Theoretical predictions from this approximate method agree with exact results in the limiting cases of zero inter-channel coupling and strong coupling. To check the overall validity of our approach for intermediate couplings, we performed extensive Monte Carlo computer simulations.



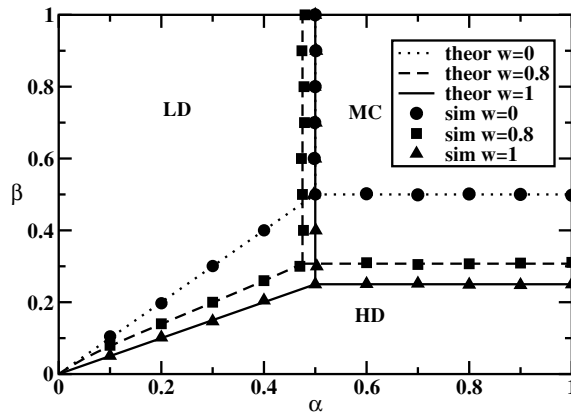


**Figure 3.** Phase diagrams for two-channel TASEPs for different inter-channel couplings. Symbols correspond to Monte Carlo computer simulations, lines are our theoretical predictions.

Our theoretical arguments are valid only in the thermodynamic limit, i.e.,  $L \rightarrow \infty$ . It means that we predict the bulk values of parameters and we mainly neglect the finite-size effects in the simplest approximation. However, in our simulations the lattice of size  $L = 100$  was used, and we checked that for larger lattices there is no difference with reported results. The density profiles and particle currents in our simulations were calculated by averaging over  $10^8$ – $10^{10}$  Monte Carlo steps, although the first 5% of the total number of steps were neglected to ensure that the system had reached the stationary state.

Boundaries in phase diagrams were determined by comparing density profiles and changes in the particle current. Specifically, the boundary between the high-density and low-density phases is observed when the density profiles are becoming linear. In this case, the visual inspection of the density profiles allows us to localize the transition line to within 0.01 units for numerical values of  $\alpha$  and  $\beta$ . The transitions between the high-density/low-density phase and the maximal-current phase are determined by observing the saturation of the particle current at specific values of  $\alpha$  or  $\beta$ . The error in calculating the phase boundaries by this method is less than 5%.

Phase diagrams and density profiles calculated from Monte Carlo simulations are presented in figures 3 and 4. The agreement with theoretically calculated values is excellent. The theoretical predictions for phase boundaries coincide with the values calculated from computer simulations; see figure 3. Similarly, the predicted bulk values of density profiles agree with Monte Carlo simulation results, as shown in figure 4. The deviations from the bulk values in density profiles are observed near the boundaries. These deviations are small in low-density and high-density phases, where the system relaxes to the bulk values exponentially fast [1, 2], while in the maximal-current phase the deviations are large since the relaxation has a power-law dependence [1, 2]. It should be noted that the phase boundary between the low-density and the high-density phases for intermediate coupling (for  $0 < w < 1$ ) deviates slightly from linear relation, in agreement with theoretical predictions. This can be seen by analysing the slope of the curve. It equals to 1 at small  $\alpha$  and  $\beta$  and slowly decreases for higher values of parameters, as shown in figure 3. The overall effect of inter-channel couplings is the decrease in a phase volume for the high-density phases. Note that although we presented only theoretical bulk values for densities of clusters and particle densities (see figure 4), the approximate theory in principle also allows us to calculate the full density profiles.

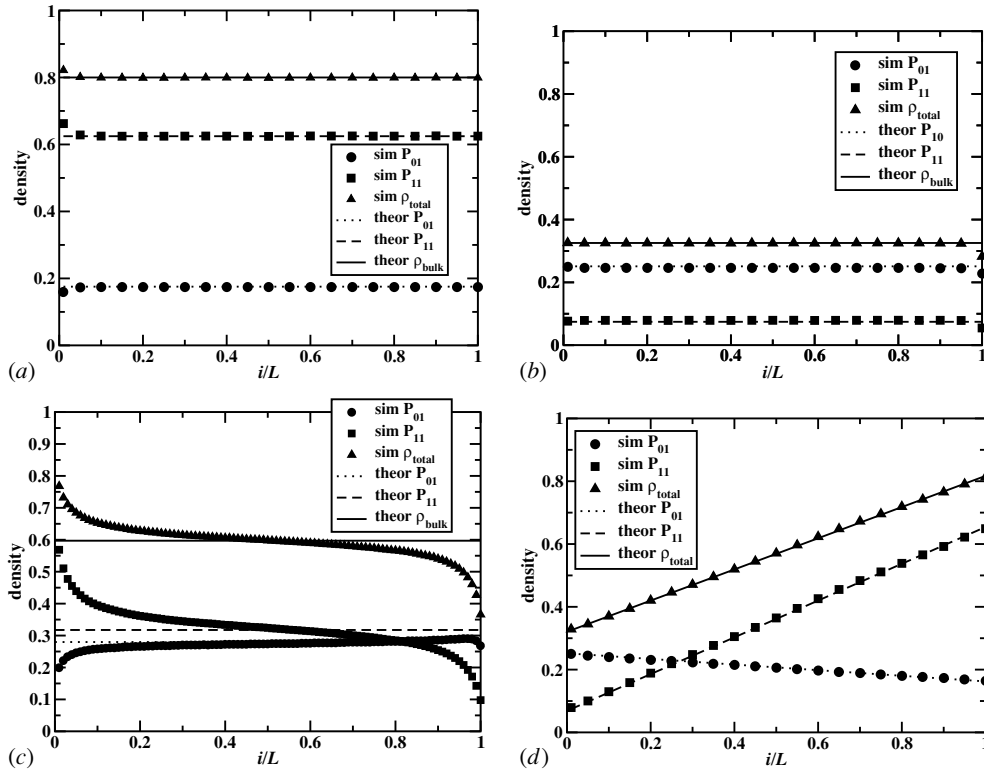


**Figure 4.** Density profiles for inter-channel coupling  $w = 0.5$ : (a) in the high-density phase with  $\alpha = 0.8$  and  $\beta = 0.2$ ; (b) in the low-density phase with  $\alpha = 0.2$  and  $\beta = 0.8$ ; (c) in the maximal-current phase with  $\alpha = 0.8$  and  $\beta = 0.8$ ; and (d) at the boundary between the low-density and the high-density phases for  $\alpha = 0.2$  and  $\beta = 0.2$ . Symbols correspond to Monte Carlo computer simulation results, lines describe theoretically calculated bulk values for  $P_{10}$ ,  $P_{11}$  and density per channel, respectively. Error bars, determined from standard deviations for simulations, are smaller than the size of the symbols.

It is interesting also to analyse the effect of inter-channel particle transitions on the dynamics of two-channel TASEPs. As shown in figure 5, the increase in inter-channel coupling generally decreases the particle current per channel, while the values of bulk densities do not change (for the high-density phase) or go up. The strongest effect is for the maximal-current and the low-density phases, while the influence of coupling on the high-density phase is quite minimal. This can be easily understood by recalling what processes determine the different steady-state phases. The entrance processes and bulk processes are strongly affected by inter-channel particle transitions, while the exit processes do not depend much on this coupling. The inter-channel coupling also has a peculiar effect on a triple point in the phase diagram, where all three phases coexist—see figure 6. The increasing inter-channel current decreases the  $\beta$ -coordinate of the triple point, while the effect on the  $\alpha$ -coordinate is non-monotonous.

In our theoretical approach, we implicitly assumed that the probability of two vertical sites to be occupied, i.e.,  $P_{11}$ , is an order parameter in the system. This assumption seems reasonable because it is rather a simple extension of the average particle density that was used as the order parameter in one-channel ASEPs.

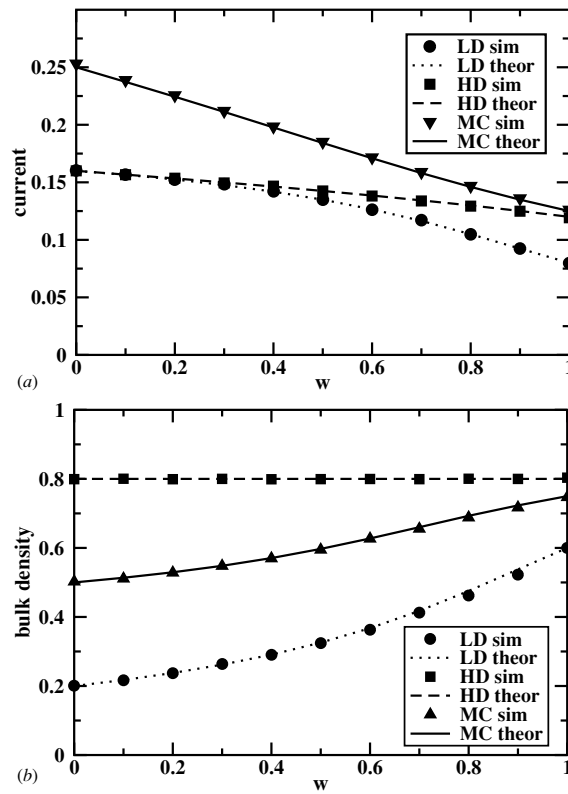


**Figure 5.** Particle currents per channel and bulk densities as a function of inter-channel coupling. The low-density phase is specified by  $\alpha = 0.2$  and  $\beta = 0.8$ ; the high-density phase is given by  $\alpha = 0.8$  and  $\beta = 0.2$ ; and the maximal-current phase is for  $\alpha = 0.8$  and  $\beta = 0.8$ . Symbols correspond to Monte Carlo computer simulations, lines are our theoretical predictions.

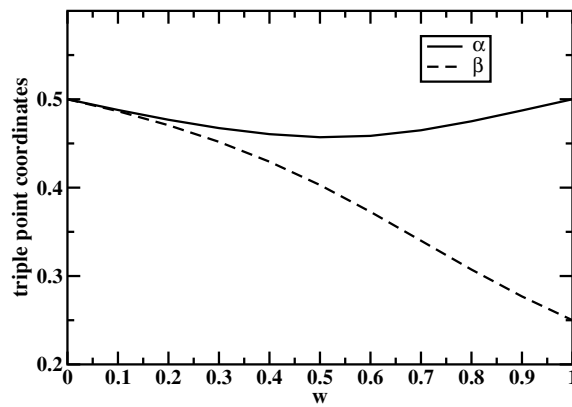


**Figure 6.** The coordinates of triple points for different inter-channel couplings. Monte Carlo computer simulation results coincide with the theoretical calculations, and thus are not shown.

#### 4. Summary and conclusions

We investigated two-channel totally asymmetric simple exclusion processes with the possibility of particle transitions between the lattice chains. When there is no coupling,  $w = 0$ , the system can be viewed as two independent one-channel TASEPs, for which exact solutions are known. In the limit of strong coupling,  $w = 1$ , the exact description of particle dynamics is obtained by mapping the two-channel system into an effective one-channel TASEP with known stationary properties.

The two-channel TASEPs with intermediate couplings are analysed with the help of an approximate theoretical approach, in which all stationary properties are obtained analytically. In our approach, the particle dynamics inside vertical clusters of corresponding lattice sites is considered exactly, while the correlations between different clusters are neglected. The results of this approximate method are in excellent agreement with Monte Carlo computer simulations. Our theoretical and computational results indicate that the inter-channel currents have a strong effect on steady-state properties of the system. Increasing the coupling lowers the particle current per channel, increases the bulk values of particle densities and shifts significantly the position of phase boundaries, although the overall topology of the phase diagram is preserved.

There are several extensions of the original two-channel TASEP that will be interesting to investigate. In this paper, we considered only the case with symmetric coupling, i.e., for any particle the probability of jumping to a different lattice chain is independent of the channel. It will be interesting to analyse the asymmetric coupling, where particles in the first channel could hop to the second channel with the rate  $w_1$ , while the opposite motion has the rate of  $w_2$ , and  $w_1 \neq w_2$ . Another more interesting, although more complex, case is the problem of non-uniform couplings between the channels. It seems reasonable to suggest that our method of combining simple approximate theory with Monte Carlo computer simulations is a promising approach to study these complex non-equilibrium one-dimensional problems.

#### Acknowledgments

The support from the Camille and Henry Dreyfus New Faculty Awards Programme (under grant no NF-00-056), from the Welch Foundation (under grant no C-1559), and from the US National Science Foundation through the grant no CHE-0237105 is gratefully acknowledged. ABK also thanks T Chou for valuable discussions.

#### References

- [1] Derrida B 1998 *Phys. Rep.* **301** 65
- [2] Schütz G M 2000 Integrable stochastic many-body systems *Phase Transitions and Critical Phenomena* vol 19 ed C Domb and J Lebowitz (London: Academic)
- [3] MacDonald J T, Gibbs J H and Pipkin A C 1968 *Biopolymers* **6** 1
- [4] Schütz G M 1999 *Europhys. Lett.* **48** 623
- [5] Chou T 1998 *Phys. Rev. Lett.* **80** 85
- [6] Widom B, Viovy J L and Defontaine A D 1991 *J. Physique I* **1** 1759
- [7] Klumpp S and Lipowsky R 2003 *J. Stat. Phys.* **113** 233
- [8] Lakatos G and Chou T 2003 *J. Phys. A: Math. Gen.* **36** 2027
- [9] Shaw L B, Zia R K P and Lee K H 2003 *Phys. Rev. E* **68** 021910
- [10] Shaw L B, Kolomeisky A B and Lee K H 2004 *J. Phys. A: Math. Gen.* **37** 2105
- [11] Kolomeisky A B, Schütz G M, Kolomeisky E B and Straley J P 1998 *J. Phys. A: Math. Gen.* **31** 6911
- [12] Parmegianni A, Franosh T and Frey E 2003 *Phys. Rev. Lett.* **90** 086601
- [13] Mirin N and Kolomeisky A B 2003 *J. Stat. Phys.* **110** 811

- 
- [14] Popkov V, Rákos A, Willmann R D, Kolomeisky A B and Schütz G M 2003 *Phys. Rev. E* **67** 066117
  - [15] Evans M R, Juhasz R and Santen L 2003 *Phys. Rev. E* **68** 026117
  - [16] Levine E and Willmann R D 2004 *J. Phys. A: Math. Gen.* **37** 3333
  - [17] Howard J 2001 *Mechanics of Motor Proteins and the Cytoskeleton* (Sunderland, MA: Sinauer Associates)
  - [18] Popkov V and Peschel I 2001 *Phys. Rev. E* **64** 026126
  - [19] Popkov V and Schütz G M 2003 *J. Stat. Phys.* **112** 523
  - [20] Popkov V 2004 *J. Phys. A: Math. Gen.* **37** 1545